The Company of **Biologists**

RESEARCH ARTICLE

Specialized landing maneuvers in Spix's disk-winged bats (*Thyroptera tricolor*) reveal linkage between roosting ecology and landing biomechanics

David B. Boerma[1,*], José P. Barrantes[2], Charles Chung[3], Gloriana Chaverri[4,5] and Sharon M. Swartz[1,6]

ABSTRACT

Disk-winged bats (*Thyroptera* spp.) are the only mammals that use suction to cling to smooth surfaces, having evolved suction cups at the bases of the thumbs and feet that facilitate attachment to specialized roosts: the protective funnels of ephemeral furled leaves. We predicted that this combination of specialized morphology and roosting ecology is coupled with concomitantly specialized landing maneuvers. We tested this by investigating landings in *Thyroptera tricolor* using high-speed videography and a force-measuring landing pad disguised within a furled leaf analogue. We found that their landing maneuvers are distinct among all bats observed to date. Landings comprised three phases: (1) approach, (2) ballistic descent and (3) adhesion. During approach, bats adjusted trajectory until centered in front of and above the landing site, typically the leaf's protruding apex. Bats initiated ballistic descent by arresting the wingbeat cycle and tucking their wings to descend toward the leaf, simultaneously extending the thumb disks cranially. Adhesion commenced when the thumb disks contacted the landing site. Significant body reorientation occurred only during adhesion, and only after contact, when the thumb disks acted as fulcra about which the bats pitched 75.02±26.17 deg (mean±s.d.) to swing the foot disks into contact. Landings imposed 6.98±1.89 bodyweights of peak impact force. These landing mechanics are likely to be influenced by the orientation, spatial constraints and compliance of furled leaf roosts. Roosting ecology influences critical aspects of bat biology, and taken as a case study, this work suggests that roosting habits and landing mechanics could be functionally linked across bats.

KEY WORDS: Biomechanics, Bat flight, Roosting ecology, Landing maneuvers, Adhesion

INTRODUCTION

Ecology provides the environmental context for evolution: shifts in ecological factors impose selective pressures on the functional systems of organisms, which can lead to reproductive isolation and eventually to speciation (Langerhans and Riesch, 2013; Schluter, 2009). Selection acts primarily upon organismal performance, and at the organism level, variation in performance often arises from variation in mechanical function, nested within which is variation in morphology and physiology (Higham et al., 2016). In some cases, a high degree of ecological specialization might also lead to concomitant specialization in movement mechanics. We explore this prediction in bats by probing the linkage between bat roosting ecology and bat landing mechanics using *Thyroptera tricolor* – a species with highly derived roosting habits – as a case study.

In bats, few aspects of ecology exert as broad an influence over other traits as their roosting habits. Bat roosts not only function as refugia from climate and predation, but also determine proximity to foraging grounds and mates, influence species assemblage composition and dispersal, provide spaces for rearing pups, and act as social hubs that facilitate food sharing and information transfer (see Altringham, 2011; Kunz and Fenton, 2006 for review). In certain cases, highly specialized roosting ecology has led to the evolution of specialized morphological structures, a phenomenon that is most evident in bats that habitually roost within tubular vegetation. This behavior has independently evolved multiple times in bats and includes species that roost within pitcher plants (Schöner et al., 2017), bamboo culms (Thewissen and Etnier, 1995) and the protective funnels of ephemeral furled leaves (Findley and Wilson, 1974; Ralisata et al., 2010). In all cases, bats with this distinctive roosting ecology have also evolved enlarged or modified regions of the integument at the bases of the thumbs and plantar surfaces of the feet that provide varying degrees of adhesion to the smooth surface of the vegetation. These adhesive pads augment and in some cases replace claw interlocking as the primary mechanism of attachment to the roost.

The bat genus *Thyroptera* currently includes five species (Velazco et al., 2014), all of which possess adhesive disks that provide attachment to smooth leaves. Investigations into the mechanism of attachment in *T. tricolor*, which roosts head-up within tubular, furled leaves (Fig. 1), demonstrated that the disks adhere via suction (Riskin and Fenton, 2001; Schliemann, 1970a,b; Schliemann and Goodman, 2011; Wimsatt and Villa-R, 1970). Suction differs from other mechanisms of adhesion in that a partial vacuum between the sucking organ and the substrate provides the adhesive force, rather than van der Waals forces or capillary action. Suction therefore requires an uninterrupted seal between the adhesive structure and nonporous substrate. Histological studies of the suction disks in *T. tricolor* provide clear evidence that they fulfill both of these requirements. The disks are continuous with the integument of the thumb or foot, are concave and are permanently moist along the ventral contact surface (Dobson, 1876; Wimsatt and Villa-R, 1970). An internal fibrocartilaginous network supports the disk's cuplike shape, while an array of sudoriparous glands along the disk rim maintain its surface moisture. The suction cups possess no intrinsic musculature, instead relying on extrinsic muscles of the

[1]Department of Ecology and Evolutionary Biology, Brown University, Providence, RI 02906, USA. [2]Escuela de Ciencias de la Computación e Informática, Universidad de Costa Rica, San José 11501, Costa Rica, USA. [3]The Peddie School, Hightstown, New Jersey 08520, USA. [4]Recinto de Golfito, Universidad de Costa Rica, Golfito 60701, Costa Rica, USA. [5]Smithsonian Tropical Research Institute, Apartado 0843–03092, Balboa, Ancón, República de Panamá. [6]School of Engineering, Brown University, Providence, RI 02906, USA.

*Author for correspondence (david_boerma@brown.edu)

D.B.B., 0000-0002-9598-5855; G.C., 0000-0002-1155-432X; S.M.S., 0000-0001-5762-7435
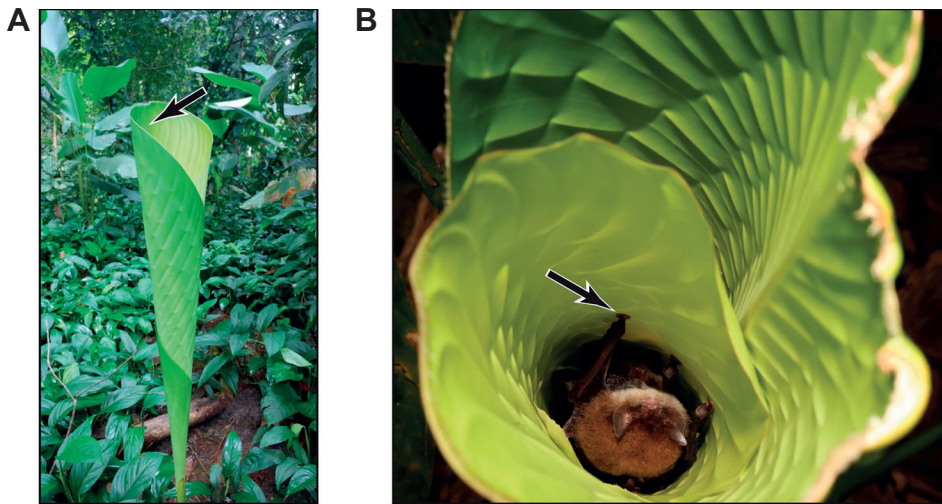
Fig. 1. Photographs of a furled leaf and roosting *Thyroptera tricolor*. (A) A furled *Heliconia* leaf, with its apex (typical landing site) indicated by the black arrow. Photo credit: D.B.B. (B) *T. tricolor* roosting within a furled leaf with an adhered thumb disk indicated by the black arrow. Photo credit: Michael Schöner.

fore- and hindlimb that insert on the fibrocartilaginous plate to provide the force required to reduce air pressure within the suction cup (Wimsatt and Villa-R, 1970).

Alongside the acquisition of these suction disks, the specialized roosting ecology of *T. tricolor* may also have influenced the mechanics of its landing maneuvers, which have yet to be formally described. Qualitative field observations describe *T. tricolor* circling furled leaves before entering the protective funnel (Findley and Wilson, 1974), but provide negligible insight into the details of their landing mechanics. Such detailed descriptions are available for three bat species that roost beneath horizontal structures, such as cave ceilings and foliage, and provide suitable metrics for assessing landing behavior and performance in *T. tricolor*. These species perform one of at least two distinct landing maneuvers that may have evolved in response to roost compliance (Riskin et al., 2009). Each landing style is named according to the number of points of contact the bat uses to gain purchase on its roost. Two-point landings require complex rotations that completely invert the bat's body prior to contact so that bats use only the hindlimbs to land with low (<2 bodyweights) peak impact forces. By contrast, four-point landings are rotationally simple, requiring only that the bats pitch backwards to orient both thumbs and both hindlimbs toward the landing site; however, four-point landings result in high impact forces (>4 bodyweights). Riskin et al. (2009) proposed that interspecific differences in landing style might be explained by roost compliance, because bats in the study that use two-point landings (*Carollia perspicillata* and *Glossophaga soricina*) habitually roosted on stiff surfaces, such as caves or tree hollows, where low-impact landings might prevent injury, whereas the species that uses four-point landings (*Cynopterus brachyotis*) roosted on compliant foliage, which could absorb the high impact forces measured by the (rigid) force plate.

T. tricolor provides a case study with which to test the prediction that landing mechanics and roosting ecology are functionally linked. We predict that its specialized roosting behavior (head-up posture within furled leaves) along with its specialized morphology (suction disks) are connected with concomitant specializations in its landing maneuvers compared with other bats. Specifically, we predict that *T. tricolor* performs a rotationally simple maneuver that primarily involves body pitch to rotate its body approximately 90 deg from a horizontal flight orientation to a head-up, vertical roosting orientation. Additionally, we predict that *T. tricolor* will enact landings at

high peak impact forces when measured with a rigid force platform. In this study, we test these predictions by using high-speed videography to record wild-caught *T. tricolor* landing on a force plate disguised as a furled leaf tube.

MATERIALS AND METHODS
Focal species, field site and animal capture
Our focal species was *Thyroptera tricolor* Spix 1823 (Wilson and Findley, 1977). We captured bats during the daytime directly from their leaf roosts, taking care to keep individuals of each group (i.e. individuals roosting in the same leaf) together. After completing experiments, we returned each group to the leaf from which they were captured. We recorded landings from adult males and nonpregnant/nonlactating females. We avoided using juveniles because they were less adept at landing both within natural leaves and our leaf analogue. We distinguished juveniles by inspecting the interphalangeal joints for degree of ossification, a morphological indicator of physical maturity. We conducted all experiments at the Hacienda Barú Biological Research Station in Puntarenas, Costa Rica. This study was approved by the Brown University IACUC and was conducted in accordance with the ethical standards for animal welfare of the Costa Rican Ministry of Environment and Energy, Sistema Nacional de Áreas de Conservación, permit no. SINAC-ACOPAC-PI-008–2017.

Experimental design and animal training
We performed landing experiments in a 3.5×2×1.5 m (L×W×H) mesh flight cage, and used high-speed videography and a force plate disguised as a furled leaf to record body movements and landing impact forces (Fig. 2, Movie 1). We recorded videos using a synchronized array of three high-speed cameras (Phantom Miro 340, Vision Research, Wayne, New Jersey, USA; 600 frames per second; 300 µs exposure; lenses: Sigma DC 17–50 mm 1:28 EX HSM) and three LED lights (Veritas Constellation 120, Integrated Design Tools, Pasadena, CA, USA). Videos were undistorted and calibrated using a checkerboard (8×6 sq., 20 mm per side) and the light video calibration routine in XMALab (Knörlein et al., 2016). We recorded calibration images at the beginning and end of each data collection session, and after accidental camera movement. We recorded landing impact forces using a force/torque transducer (ATI Nano17, ATI Industrial Automation, Apex, NC, USA) fitted with custom acrylic mounting and landing plates (1000 Hz sampling frequency).
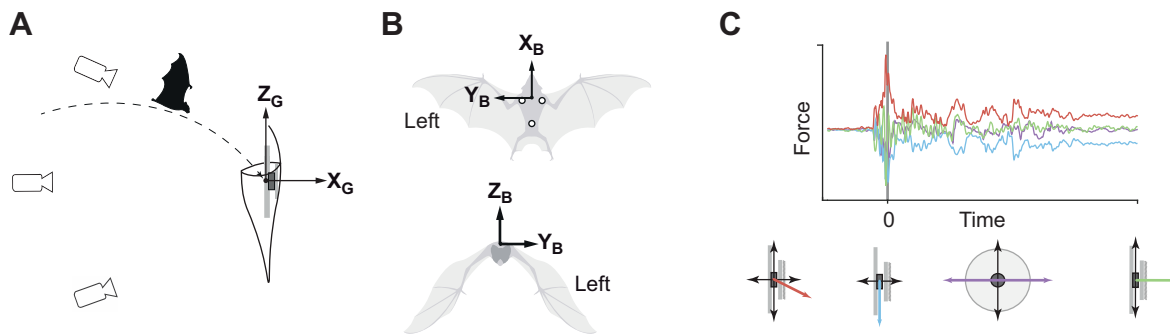
Fig. 2. Experimental design. (A) Bats were trained to land on a vertically mounted force plate disguised as a furled leaf and landings were recorded using three high-speed cameras. We used the plate axes to define a global coordinate system [X_G,Y_G,Z_G]; +Y_G (not pictured) points away from the viewer. (B) We placed anatomical landmarks on the shoulders and the lower back. We used these points to approximate body position and define a body-referenced coordinate system [X_B,Y_B,Z_B] for calculating body orientation. (C) Representative force profile and plate axes. We extracted peak impact forces (time=0) in each axis, total impact (red), vertical (blue), lateral (purple) and normal (green).

T. tricolor readily landed in leaf analogues made from thin plastic. We therefore mounted the landing pad to a rigid vertical surface, and disguised it as a furled leaf by surrounding it with a funnel of thin, clear plastic. We positioned the landing pad within the funnel, beneath the pointed apex, the location within natural leaves where *T. tricolor* typically lands (field observations, G.C., J.P.B., E. Gillam and D.B.B.) (Fig. 1A and Fig. 2A).

We trained each bat by releasing it into the flight cage and allowing it to fly undisturbed until it landed within the false leaf. Bats were free to approach the leaf from any angle and often encircled the leaf one to three times before landing beneath the leaf's pointed apex, a behavior reported for wild *Thyroptera* landing in natural leaves within the forest (Findley and Wilson, 1974). Once the bat landed, we allowed it a 3 min rest within the leaf before removing and re-releasing it within the enclosure, and commenced data collection after three successful training landings. It is possible that this training allowed the bats to adjust their landing dynamics compared with landing on softer natural leaves, but qualitative comparisons between landing on the rigid force plate and landing on a natural leaf do not reveal obvious differences in landing phases, points of contact or body rotations (see Movies 2 and 3). Any adjustments are likely to be subtle and their description requires detailed analysis of landings on surfaces more compliant than our rigid landing plate. Additionally, in 10 out of 11 individuals with ≥3 landings, repeated landings on the rigid plate did not lead to systematic changes in the magnitude of landing impact forces. We weighed each bat using a 10 g Pesola scale prior to experimental trials and recorded up to five landings per individual.

Marker tracking, coordinate systems and kinematic calculations

We marked the shoulders and the dorsal midline above the sacrum ('lumbar' marker) using white DecoColor fine line opaque paint markers (Fig. 2C). Paint marks were approximately circular and ≤3 mm in diameter. We calculated 3D coordinates for each landmark from the calibrated landing videos of the three camera views using the open-source motion tracking software XMALab (Knörlein et al., 2016). We calculated all kinematic measurements relative to a global coordinate system defined by the landing plate axes. In this plate coordinate system, +Z_G was directed vertically upwards with respect to gravity, +Y_G was directed to the bat's left as it approached the plate, and +X_G was normal to the plate. The plate center defined the origin of this global coordinate system. We used

the anatomical landmarks to define a body-referenced coordinate system [X_B,Y_B,Z_B] (Fig. 2B), with its origin [0,0,0] at the midpoint between the shoulders. X_B was oriented by a vector from the lumbar marker to the inter-shoulder point (+X_B=cranial), Z_B was orthogonal to X_B and a vector from the right to the left shoulder (+Z_B=dorsal) and Y_B was orthogonal to X_B and Z_B (+Y_B=lateral, toward the bat's left).

We approximated the position of the bat's body relative to the plate center using the average position of the left and right shoulders and the lumbar marker. Prior to averaging, we smoothed position data for the shoulders and lumbar markers using a zero-phase 2nd order low-pass Butterworth filter with a cut-off frequency of 40 Hz, 4–5 times greater than the wingbeat frequency. We then calculated 3D position of this mean body marker relative to the global origin (plate center). We acquired measurements of body velocity in each global axis independently by iteratively fitting a first-order polynomial to the body position over a sliding interrogation window of nine frames and calculating the first derivative. We followed the same procedure to acquire measurements of body acceleration from the first derivative of body velocity. We then calculated body speed as the magnitude of the 3D velocity vector.

We describe the bat's orientation in terms of pitch, yaw and roll angles, which we calculated using the Euler rotation sequence required to align the global coordinate system [X_G,Y_G,Z_G] with the body-referenced coordinate system [X_B,Y_B,Z_B]. We calculated these angles in the order of pitch, yaw, then roll so that our results would be comparable with existing measurements for bat landings (Riskin et al., 2009). Although these values are traditionally calculated in the order yaw, pitch, then roll (Stengel, 2015), this traditional order results in discontinuities in measured angles for bat landings in other species that fully invert their bodies to land, such as those described in Riskin et al. (2009). In our framework, a bat at [0 deg pitch, 0 deg yaw, 0 deg roll] would be positioned at the plate center, horizontal with respect to gravity, with [X_B,Y_B,Z_B] aligned with [X_G,Y_G,Z_G]. The reader may note that in our coordinate system, a positive pitching rotation would depress the head and elevate the feet; therefore for ease of interpretation, we multiplied all pitching rotations by −1 so that increasing pitch values correspond with increasingly elevating the head relative to the feet.

For all 44 landings (*n*=14 individuals), we calculated instantaneous body orientation at four key moments during the landing maneuver (wing tuck, first thumb contact, second thumb contact, and the settled

posture at the end of landing). For a subset of 10 landings (n=10 individuals), we calculated time-series body position, orientation, speed, and acceleration for the entire landing maneuver.

Impact force analysis

Our force plate recorded impact force in each of the three global axes at a frequency of 1000 Hz. We filtered force data using a zero-phase 2nd order low-pass Butterworth filter with a cut-off frequency of 100 Hz. This filtering attenuates high-frequency oscillations and electrical noise while preserving the primary peaks associated with landing impact. Although filtering diminishes the absolute magnitude of these force peaks, thus underestimating impact force magnitude, accurate comparisons among individuals and among force components are preserved (Riskin et al., 2009, Fig. S1). Our selection of a 100 Hz cut-off frequency permits direct comparison with published landing impact forces from three additional species described in Riskin et al. (2009). We normalized impact forces to each individual's bodyweight, then extracted peak 3D impact force ($\mathbf{F_{tot}}$), along with its components: peak vertical force ($\mathbf{F_x}$), peak lateral force ($\mathbf{F_y}$), and peak normal force ($\mathbf{F_z}$) (Fig. 1C).

Statistics

We used R v.3.4.0 (https://www.r-project.org/) to compute summary statistics and conduct all statistical tests. We recorded 44 landings from 14 individuals. We calculated individual means (n=14) for each variable except for body speed and acceleration, assessed for normality using a Shapiro–Wilk normality test, and log-transformed non-normal data prior to statistical tests. We calculated body speed and acceleration over time for a subset of 10 trials, each from a different individual (n=10). We used model II ranged major axis linear regression, as implemented in the R package *lmodel2* (https://cran.r-project.org/web/packages/lmodel2) to explore the relationships between peak 3D landing impact force and fourteen kinematic measurements, including body positions and average velocities at key moments during the landing maneuver and the duration of wing tucking prior to contact. Because no measured variables were significantly correlated with peak 3D landing impact force, we provide a

summary of this analysis in Fig. S2. Unless otherwise indicated, we report all measurements as means±s.d. (n=14).

## RESULTS

Landing maneuver sequence

All *T. tricolor* executed landing maneuvers that comprised three phases: (1) approach, (2) ballistic descent and (3) adhesion (Fig. 3). During the approach phase, bats flew toward the leaf tube opening, choosing either to approach from directly the front of the leaf tube or by circling around the leaf tube before transitioning to the descent phase. Once centered in front of and slightly above the leaf opening, bats then arrested their wingbeat cycle and retracted both wings to initiate the ballistic descent phase (Fig. 3B). During descent, bats maintained horizontal body orientation and kept both wings folded with thumbs extended cranially. They achieved this wing posture, hereafter referred to as wing tucking, primarily by folding the handwing via wrist flexion while extending the wings cranially via humeral abduction and elbow extension. They then initiated the adhesion phase upon contact with the landing plate (Fig. 3C). In 35 out of 44 landings, the thumb disks were the first two points of attachment and acted as fulcra about which the bat rotated to swing the foot disks into contact with the landing plate. In 9 out of 44 landings, however, one thumb disk either failed to adhere or never made contact; in these cases, limb contact order was thumb–foot–foot.

Body position, speed and acceleration

The three landing maneuver phases corresponded with particular body positions, velocities and accelerations (Fig. 4). In a typical landing, bats negotiated the approach phase by flying toward the landing site until they were 0.53±2.98 cm left–right of center and 6.41±1.64 cm above the landing plate center. Mean speed and acceleration during the approach phase were 0.81±0.15 m s^{-1} and 14.41±3.21 m s^{-2}. Once bats were 10.36±1.71 cm (total distance) from the plate center, they tucked their wings to initiate ballistic descent. Descent was characterized primarily by decreasing elevation, with mean speed of 0.97±0.15 m s^{-1} and acceleration of 12.83±3.87 m s^{-2}, near that of gravity. The adhesion phase began at the moment of first contact between the bat and the landing plate.
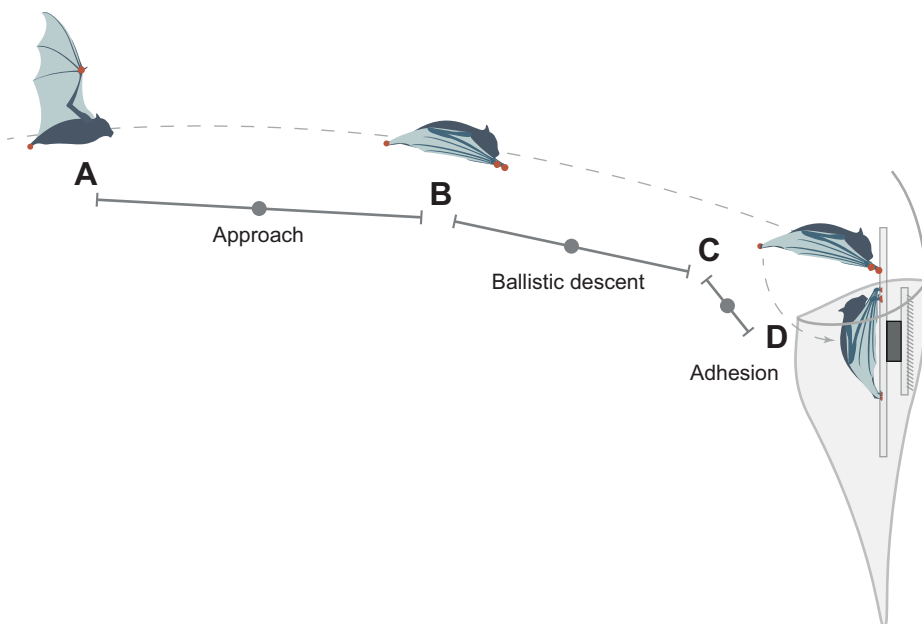
Fig. 3. Landing maneuver sequence of *T. tricolor* on a furled leaf. (A) The bat positions itself in front of and above the landing plate during the approach phase. (B) The bat tucks its wings to begin the ballistic descent phase. (C) The bat initiates contact with the landing plate to begin the adhesion phase. (D) A fully adhered bat at the conclusion of its landing maneuver.
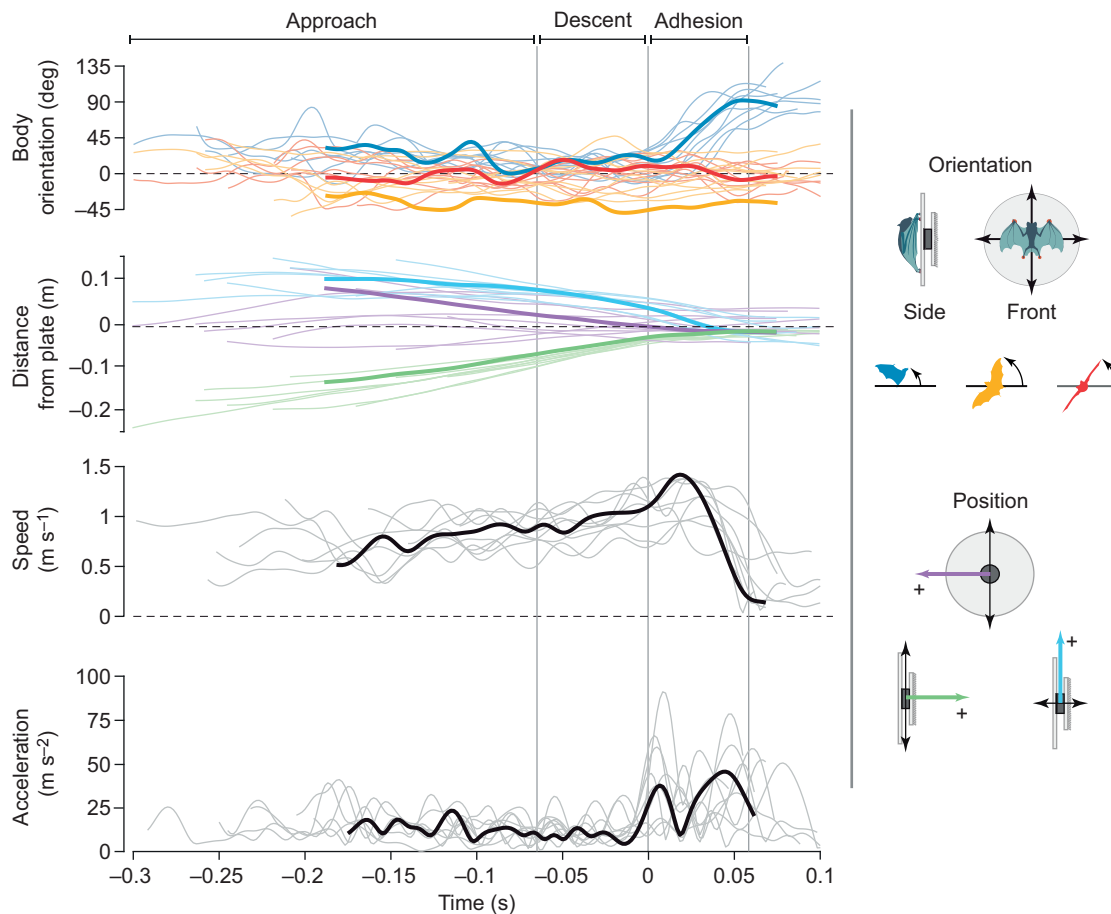
Fig. 4. Kinematic measurements from landing maneuvers. Vertical lines mark the approximate timing of transitions between landing phases across trials (approach, descent and adhesion). Time series curves show body orientation, body position relative to the landing plate center, body speed and body total acceleration. The orientation key (top right) depicts a bat at [pitch=90 deg, yaw=0 deg, roll=0 deg] orientation: adhered, head-up, to the plate center. Legends for pitch (blue), yaw (gold), and roll (red) are provided below. The position key (bottom right) show the reference frame for body position relative to the plate center. Plate axes in front (top) and side (bottom) views are left–right of center (purple), normal (green) and vertical (blue). These axes correspond to the body position measurements shown in the plot. n=10 individuals, with one representative trial shown in bold.

Bats did not decelerate prior to contact, which occurred at 1.27 ±0.17 m s^{-1}.

Body reorientation

Throughout the landing maneuver, bats exerted control not only over their position relative to the landing plate, but also over their body orientation (Figs 4 and 5). During approach, body roll remained near zero, while yaw values, which reflected whether the bat's heading was pointing left or right, remained relatively constant. Body pitch angles decreased until bats were approximately horizontal (instantaneous orientation at initiation of ballistic descent: −0.31±10.56 deg roll; 11.98±14.04 deg pitch; −7.01±16.73 deg yaw), at which point they tucked their wings to begin ballistic descent. Body orientation did not change significantly during descent, with bats making contact at 1.63±8.37 deg roll; 13.56±12.22 deg pitch; −9.73±17.78 deg yaw (Welch two-sample t-test, orientation at wing tuck vs. contact: t_{roll}=−0.537, df$_{roll}$=24.705, P_{roll}=0.596; t_{pitch}=−0.318, df$_{pitch}$=25.522, P_{pitch}=0.753; t_{yaw}=0.417, df$_{yaw}$=25.903, P_{yaw}=0.680). Once bats initiated adhesion at contact, however, the thumbs acted as fulcra about which the bats rotated, effecting significant changes in only body pitch (difference between body pitch at the beginning and end of adhesion phase: 75.02±26.17 deg), terminating in a head-up posture (Welch two sample t-test, orientation at beginning vs. end

of adhesion phase: t_{roll}=1.970, df$_{roll}$=24.938, P_{roll}=0.060; t_{pitch}=−14.716, df$_{pitch}$=24.941, P_{pitch}=8.418×10^{-14}; t_{yaw}=0.362, df$_{yaw}$=25.890, P_{yaw}=0.721).

Peak landing impact forces

Thyroptera landings resulted in high impact forces. Mean peak total impact force ($\mathbf{F_{tot}}$) was 6.98±1.89 bodyweights (BW), with large downward and forward components. Peak vertical force, $\mathbf{F_x}$, was 5.08±1.81 BW, and was oriented downward; peak normal force, into the plate, $\mathbf{F_z}$, was 4.87±1.86 BW; and the peak lateral (left–right) force, $\mathbf{F_y}$, was 1.06±0.84 BW (Fig. 6).

DISCUSSION

Analysis of high-speed video and landing impact forces of more than 40 landings from >12 individual *T. tricolor* shows that landing maneuvers are accomplished primarily by pitching the body and proceed through a sequence comprising three phases: (1) approach, (2) ballistic descent and (3) adhesion (Fig. 3). During approach, bats flew toward the leaf tube opening until they were centered in front of and slightly above the landing target (force plate), with the vertebral column oriented parallel to the ground and the head pointing toward the force plate. Once bats reached this position and orientation, they tucked their wings to begin ballistic descent, during which body orientation and speed remained relatively constant, and
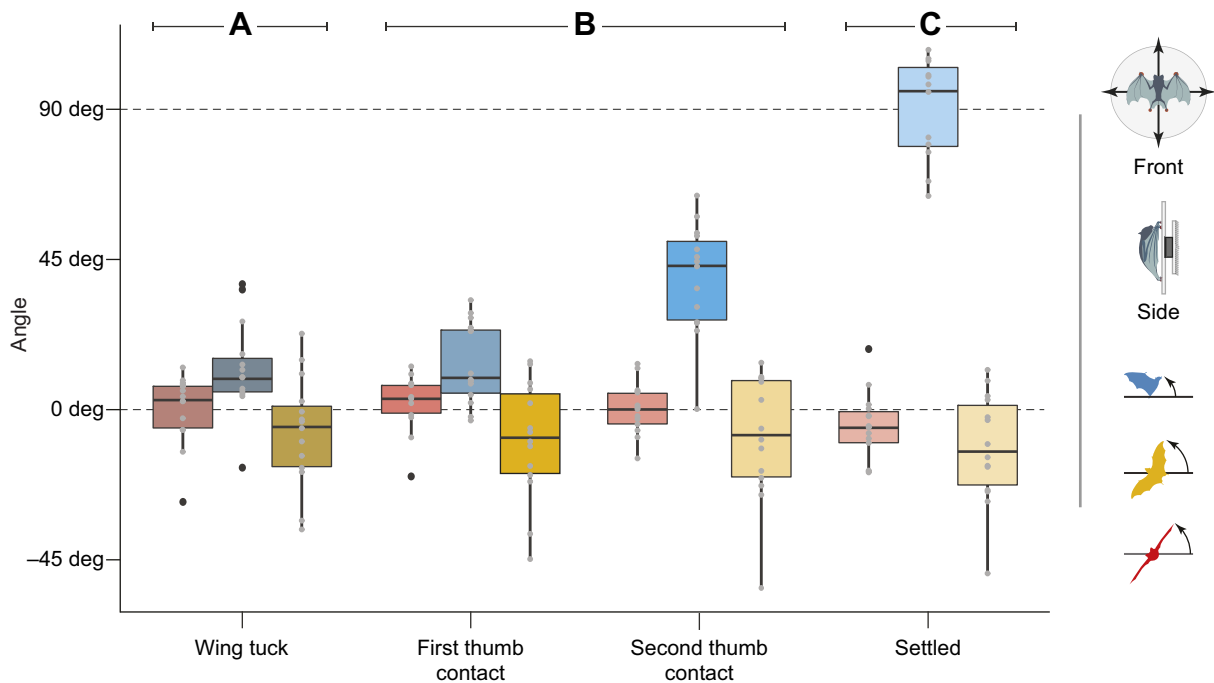
Fig. 5. Instantaneous body orientation at four key moments during the landing maneuver. Pitch (blue), yaw (gold) and roll (red) angles for each instance are represented visually by changes in color tint, from darker to lighter: (i) wing tuck, (ii) first thumb contact, (iii) second thumb contact and (iv) settled (*n*=14 individuals; individual data points in gray). (A) The beginning of ballistic descent. (B) The adhesion phase. (C) The 'settled' posture after bats complete a landing shown in the orientation key (right). A bat at [0,0,0] orientation would be oriented horizontal relative to the external environment. Box plots show the median (horizontal line) and interquartile range (upper and lower bounds of the box); outliers indicated by black points.

acceleration was near that of gravity. Bats transitioned from descent to adhesion upon making contact with the landing plate using the suction cups at the bases of the thumbs. With both thumbs adhered to the plate, these first points of attachment acted as fulcra about which the bats pitched to swing the foot suction cups into contact with the plate. Landings imposed high impact forces, with bats sustaining average peak impact forces of nearly seven times their bodyweight.

Roosting ecology as the driver of specialized landing maneuvers in *Thyroptera tricolor*

Bat species that land on the underside of horizontal surfaces (e.g. cave ceilings, tree hollows and foliage) have been described as using one of at least two known landing maneuvers, which can be named according to the number of limbs that make initial contact at landing impact with the roost: two-point and four-point landings (Riskin et al., 2009). *T. tricolor* landings differed from
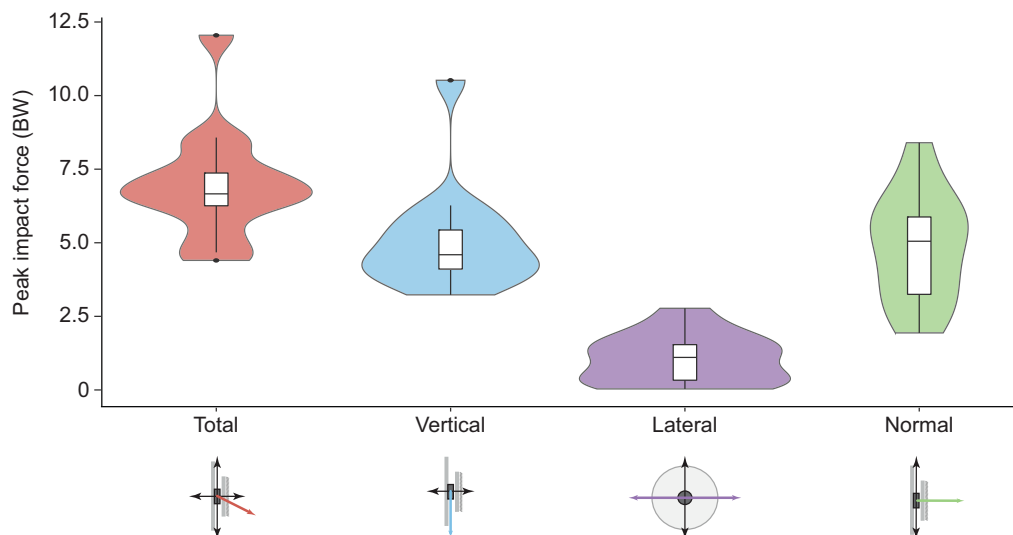
Fig. 6. Peak impact forces. The absolute values of peak forces are normalized to bodyweight, for total 3D impact force (red), the vertical component (blue), lateral (left–right) component (purple), and normal component (green). Box plots show the median (horizontal line) and interquartile range (upper and lower bounds of white box). Colored envelopes surrounding boxplots provide a visualization of the distribution of data within the boxes (*n*=14 individuals).

these previously described maneuvers in (1) the timing and magnitude of body rotations and (2) the magnitude of peak landing impact forces.

Like *T. tricolor*, *Cynopterus brachyotis*, a bat that uses four-point landings, reorients its body to land by modulating body pitch, with negligible contributions from body roll and yaw (Riskin et al., 2009). However, *C. brachyotis* completes the majority of its body reorientation prior to contacting the landing site. In contrast, our measurements show that *T. tricolor* does not begin to alter body pitch until after the thumb disks make contact with the landing plate, at the beginning of adhesion phase (Fig. 7). *C. brachyotis* and *T. tricolor* also differ in the final target body orientation (roosting orientation), as *T. tricolor* roosts head-up within leaf tubes rather than head-under-heels. Therefore, its landings require only 75.02±26.17 deg of body pitch during adhesion phase, the period over which significant body reorientation occurs, compared to approximately 150 deg in *C. brachyotis* (Riskin et al., 2009).

Normalized peak 3D landing impact forces were higher in *T. tricolor* than in any other bat measured to date. Four-point landings in *C. brachyotis* resulted in mean landing impact forces of 3.83±1.23 BW (Riskin et al., 2009), whereas mean landing impact forces in *T. tricolor* were 6.98±1.89 BW. These higher impact forces likely do not function to enhance suction attachment, because *T. tricolor* readily adhere and release their suction cups even in the absence of high forces, such as when crawling along the leaf surface. Rather, *Thyroptera* landings may involve higher impact forces for at least three reasons, each related to its roosting habits. First, because *T. tricolor* roosts head-up within vertical furled leaves, the bat necessarily lands on a surface positioned in front of and below it. Compared with bats that roost on ceilings, where the negative acceleration of gravity opposes the upward acceleration toward the landing site, *T. tricolor* descend as they approach their leaf landing targets, accelerating in the same direction as gravity. They thus continue to increase in speed under only partly mitigated gravitational acceleration, which can lead to comparatively higher impact forces. Second, the confined, tubular morphology of its leaf roosts may prevent *T. tricolor* from performing decelerating wingbeats prior to impact. These spatial constraints may explain why *T. tricolor* terminates the normal wingbeat cycle prior to its descent. Finally, *T. tricolor* attach to leaf surfaces via a mechanism that requires a bat to

form suction immediately upon contact with its roost surface. Although tucking its wings to descend into the leaf tube prevents the bat from using aerodynamic forces to modulate its speed prior to impact, it liberates the forelimbs from functioning as aerodynamic surfaces, thus permitting the bat to extend its suction cups toward the leaf to establish rapid adhesion. Taken together, these facets of its roosting ecology – head-up roosting posture, tubular leaf roosts and suctorial attachment – provide explanations as to why *T. tricolor* differs from other bats in its landing kinematics and landing impact forces.

Predictions for convergence in other leaf tube-roosting bats

Although multiple evolutionary solutions to ecological problems can exist (Wainwright et al., 2005), convergence in morphology, physiology or biomechanical behavior can provide strong evidence of selection in response to shared ecology. A robust test of our hypothesis that this specialized roosting ecology strongly influences landing biomechanics would be to test for convergent landing styles among species that evolved similarly derived roosting habits. To date, biologists have identified a number of bat species that habitually roost within tubular vegetation (Dobson, 1876; Goodman et al., 2007; Thewissen and Etnier, 1995; Wilson and Findley, 1977). A relatively distantly related bat that closely resembles *Thyroptera* in roosting habits and adhesive capacity is *Myzopoda aurita* (Schliemann and Maas, 1978). This species is endemic to Madagascar and independently evolved similarly effective adhesive pads that enable roosting in furled leaves. However, *M. aurita* attaches via wet adhesion rather than suction (Riskin and Racey, 2010; Schliemann, 1970b; Schliemann and Goodman, 2011). Given this striking ecological and morphological convergence, we predict that *M. aurita* has also converged upon a landing maneuver that closely resembles that of *T. tricolor* and suggest that future work seeks to test this prediction.

Many of the other bat species that share roosting habits similar to those of *T. tricolor* and *M. aurita* possess only incipient adhesive pads compared with those of the more specialized taxa (Thewissen and Etnier, 1995). These pads differ from the derived structures of *Thyroptera* and *Myzopoda* in that they possess neither a convex, cuplike structure nor the numerous glands to secrete liquid to aid in adhesion. Rather, incipient adhesive structures tend to consist of enlarged regions of integument below the thumbs and above the feet, the surfaces of which vary in their degrees of texture and glandular tissue (Schöner et al., 2017; Thewissen and Etnier, 1995). Bats with incipient pads roost in the internodes of bamboo, wedged within the helices of rolled leaves, and within pitcher plants, rather than directly on smooth leaf surfaces (Happold and Happold, 1990; Medway and Marshall, 1970; Schöner et al., 2017; Thewissen and Etnier, 1995). It has been suggested that the less-derived morphology observed in these species indicates that they have experienced a shorter period of selection for more-derived adhesive structures (Schliemann, 1970b). Future studies of landing maneuvers for these species may therefore provide a window into evolutionary intermediate stages for landing maneuvers in bats that use adhesive organs to roost in tubular foliage.

Roosting ecology as a driver of diverse landing styles across bats

Thyroptera tricolor provides an extreme example of how morphology and landing mechanics respond to specialization in roosting habits, but similar linkages among roosting ecology, wing morphology and landing style may also be present across the nearly 1400 species of bats. A broader comparative analysis of bat landings with divergent roosting ecologies and landing styles would provide a powerful framework for understanding the linkages between
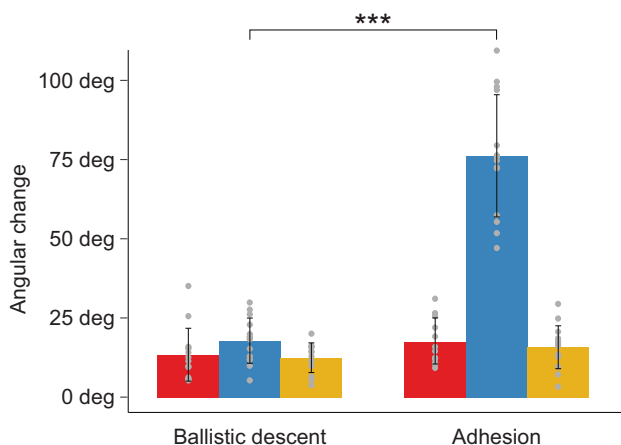
Fig. 7. Body reorientation is concentrated in the adhesion phase. Angular change calculated as the difference between the values at the end and beginning of descent phase (left) and adhesion phase (right) for body roll (red), pitch (blue) and yaw (gold) (mean±s.d., *n*=14 individuals; individual data points in gray). Significant difference in pitch only (Welch two-sample *t*-test, *P*=8.418×10⁻¹⁴).

ecology and biomechanical performance. In particular, closely related species with differing roosting habits, including other species of *Thyroptera*, which roost in dead leaves (Gregorin et al., 2006; Robinson and Lyon, 1901; Solari et al., 1999; Velazco et al., 2014), would be suitable focal taxa for testing the hypothesis that divergence in roosting ecology interacted with divergence in landing performance as bats diversified. Bats in the phyllostomid subfamily Stenodermatinae could be of particular interest. Recent work placed a shift from cavity roosting to foliage roosting at the base of this clade (Garbino and Tavares, 2018). If bat landing maneuvers evolved to modulate impact force in response to roost compliance, we would predict a shift from two-point landings to four-point landings in stenodermatines. Similarly, we would expect to find convergence of low-impact two-point landings in other bats that habitually roost on cave ceilings, such as the Rhinolophidae and Hipposideridae of Europe and East Asia. Such results would provide strong evidence of biomechanical adaptation (landing style) to a critical ecological factor (roosting habits).

In conclusion, the results of our study demonstrate that *T. tricolor* land on furled leaves by performing maneuvers that comprise three phases: (1) approach, (2) ballistic descent and (3) adhesion. These maneuvers are distinct among those described for bats in that they are the most rotationally simple landing maneuvers yet measured (primarily pitching rotations; ∼75 deg), and significant body rotation begins only after bats make contact with the landing site. These landings also result in the highest-measured normalized peak impact forces (∼7 BW). We attribute these unique qualities to pressures imposed by their highly specialized roosting ecology, including a roosting posture that requires simple rotations to achieve, spatial constraints that may prevent decelerative wingbeats and leaf compliance that may mitigate the high impact forces we measured on a rigid force plate. We hypothesize that other bats that have evolved leaf-tube roosting, particularly *M. aurita*, convergently evolved similar landing maneuvers. Taken as a case study, the concomitant specialization of roosting habits and landing mechanics in *T. tricolor* suggest that these traits might be functionally linked across bats and warrant a broader, phylogenetically informed comparative analysis to elucidate connections among ecology, morphology and movement in bats.

Author contributions
Conceptualization: D.B.B., G.C., S.M.S.; Methodology: D.B.B., J.P.B., G.C., S.M.S.; Formal analysis: D.B.B., C.C.; Investigation: D.B.B., J.P.B.; Resources: G.C., S.M.S.; Writing - original draft: D.B.B.; Writing - review & editing: D.B.B., J.P.B., C.C., G.C., S.M.S.; Supervision: G.C., S.M.S.; Funding acquisition: D.B.B.

Data availability
The data supporting this article are available from the Brown Digital Repository: https://doi.org/10.26300/jktn-sb89.

Supplementary information
Supplementary information available online at
http://jeb.biologists.org/lookup/doi/10.1242/jeb.204024.supplemental

References

Altringham, J. D. (2011). Roosting and feeding ecology. In *Bats: from Evolution to Conservation*, pp. 137-174. New York, NY: Oxford University Press.

Dobson, G. (1876). On peculiar structures in the feet of certain species of mammals which enable them to walk on smooth perpendicular surfaces. *Proc. Zool. Soc. Lond.* **44**, 526-535. doi:10.1111/j.1096-3642.1876.tb02593.x

Findley, J. S. and Wilson, D. E. (1974). Observations on the neotropical disk-winged bat, *Thyroptera tricolor* spix. *J. Mammal.* **55**, 562-571. doi:10.2307/1379546

Garbino, G. S. T. and Tavares, V. D. C. (2018). Roosting ecology of Stenodermatinae bats (Phyllostomidae): evolution of foliage roosting and correlated phenotypes. *Mamm. Rev.* **48**, 75-89. doi:10.1111/mam.12114

Goodman, S. M., Rakotondraparany, F. and Kofoky, A. (2007). The description of a new species of Myzopoda (Myzopodidae: Chiroptera) from western Madagascar. *Mamm. Biol.* **72**, 65-81. doi:10.1016/j.mambio.2006.08.001

Gregorin, R., Gonçalves, E., Lim, B. K. and Engstrom, M. D. (2006). New species of disk-winged bat *Thyroptera* and range extension for *T. discifera*. *J. Mamm.* **87**, 238-246. doi:10.1644/05-MAMM-A-125R1R1.1

Happold, D. C. D. and Happold, M. (1990). The domiciles, reproduction, social organisation and sex ratios of the banana bat *Pipistrellus nanus* (Chiroptera, Vespertilionidae) in Malawi, Central Africa. *Z. Säugetierk.* **55**, 145-160. doi:10.1515/mamm.1996.60.4.517

Higham, T. E., Rogers, S. M., Langerhans, R. B., Jamniczky, H. A., Lauder, G. V., Stewart, W. J., Martin, C. H. and Reznick, D. N. (2016). Speciation through the lens of biomechanics: locomotion, prey capture and reproductive isolation. *Proc. R. Soc. B* **283**, 20161294-39. doi:10.1098/rspb.2016.1294

Knörlein, B. J., Baier, D. B., Gatesy, S. M., Laurence-Chasen, J. D. and Brainerd, E. L. (2016). Validation of XMALab software for marker-based XROMM. *J. Exp. Biol.* **219**, 3701-3711. doi:10.1242/jeb.145383

Kunz, T. H. and Fenton, M. B. (2006). *Bat Ecology*. University of Chicago Press.

Langerhans, R. B. and Riesch, R. (2013). Speciation by selection: a framework for understanding ecology's role in speciation. *Curr. Zool.* **59**, 31-52. doi:10.1093/czoolo/59.1.31

Medway, L. and Marshall, A. G. (1970). Roost-site selection among flat-handed bats (*Tylonycteris* spp). *J. Zool.* **161**, 237-245. doi:10.1111/j.1469-7998.1970.tb02038.x

Ralisata, M., Andriamboavonjy, F. R., Rakotondravony, D., Ravoahangimalala, O. R., Randrianandrianina, F. H. and Racey, P. A. (2010). Monastic *Myzopoda*: the foraging and roosting ecology of a sexually segregated Malagasy endemic bat. *J. Zool.* **74**, 130-139. doi:10.1111/j.1469-7998.2010.00724.x

Riskin, D. K. and Racey, P. A. (2010). How do sucker-footed bats hold on, and why do they roost head-up? *Biol. J. Linnean Soc.* **99**, 233-240. doi:10.1111/j.1095-8312.2009.01362.x

Riskin, D. K. and Fenton, M. B. (2001). Sticking ability in Spix's disk-winged bat, *Thyroptera tricolor* (Microchiroptera: Thyropteridae). *Can. J. Zool.* **79**, 2261-2267. doi:10.1139/z01-192

Riskin, D. K., Bahlman, J. W., Hubel, T. Y., Ratcliffe, J. M., Kunz, T. H. and Swartz, S. M. (2009). Bats go head-under-heels: the biomechanics of landing on a ceiling. *J. Exp. Biol.* **212**, 945-953. doi:10.1242/jeb.026161

Robinson, W. and Lyon, M. W. (1901). An annotated list of mammals collected in the vicinity of La Guaira, Venezuela. *Proc. U. S. Natl. Mus.* **24**, 135-162. doi:10.5479/si.00963801.1246.135

Schliemann, H. (1970a). Bau und funktion der haftorgane von Thyroptera und Myzopoda (Vespertilionoidea, Microchiroptera, Mammalia). *Z. Wissenschaftliche Zool.* **181**, 353-400. doi:10.1111/j.1439-0469.1971.tb00887.x

Schliemann, H. (1970b). Die haftorgane von Thyroptera und Myzopoda (Microchiroptera, Mammalia) — gedanken zu ihrer entstehung als parallelbildungen. *Z. Zool. Syst. Evol.* 61-80. doi:10.1111/j.1439-0469.1971.tb00887.x

Schliemann, H. and Maas, B. (1978). *Myzopoda aurita. Mamm. Species* **116**, 1-2. doi:10.2307/3504052

Schliemann, H. and Goodman, S. M. (2011). A new study on the structure and function of the adhesive organs of the Old World sucker-footed bat (*Myzopoda*: Myzopodidae) of Madagascar. *Verh. Naturwissenschaftlichen Ver. Hamburg* **46**, 313-330.

Schluter, D. (2009). Evidence for ecological speciation and its alternative. *Science* **323**, 737-741. doi:10.1126/science.1160006

Schöner, M. G., Schöner, C. R., Kerth, G., Suhaini, S. N. B. P. and Grafe, T. U. (2017). Handle with care: enlarged pads improve the ability of Hardwicke's woolly bat, *Kerivoula hardwickii* (Chiroptera: Vespertilionidae), to roost in a carnivorous pitcher plant. *Biol. J. Linn. Soc.* **122**, 643-650. doi:10.1093/biolinnean/blx098

Solari, S., Pacheco, V. and Vivar, E. (1999). Nuevos registros distribucionales de murciélagos peruanos. *Rev. Per. Biol.* **6**, 152-159. doi:10.15381/rpb.v6i2.8310

Stengel, R. F. (2015). *Flight Dynamics*. Princeton University Press.

Thewissen, J. G. M. and Etnier, S. A. (1995). Adhesive devices on the thumb of Vespertilionoid bats (Chiroptera). *J. Mammal.* **76**, 925. doi:10.2307/1382762

Velazco, P. M., Gregorin, R., Voss, R. S. and Simmons, N. B. (2014). Extraordinary local diversity of disk-winged bat (Thyropteridae: *Thyroptera*) in

Northeastern Peru, with the description of a new species and comments on roosting behavior. *Am. Mus. Novit.* **2014**, 1-28. doi:10.1206/3795.1

Wainwright, P. C. P., Alfaro, M. E. M., Bolnick, D. I. D. and Hulsey, C. D. C. (2005). Many-to-one mapping of form to function: a general principle in organismal design? *Integr. Comp. Biol.* **45**, 256-262. doi:10.1093/icb/45.2.256

Wilson, D. E. and Findley, J. S. (1977). *Thyroptera tricolor*. *Mamm. Spec.* **71**, 1-3. doi:10.2307/3503885

Wimsatt, W. A. and Villa-R, B. (1970). Locomotor adaptations in the disc-winged bat *Thyroptera tricolor*. I. functional organization of the adhesive discs. *Am. J. Anat.* **129**, 89-119. doi:10.1002/aja.1001290107
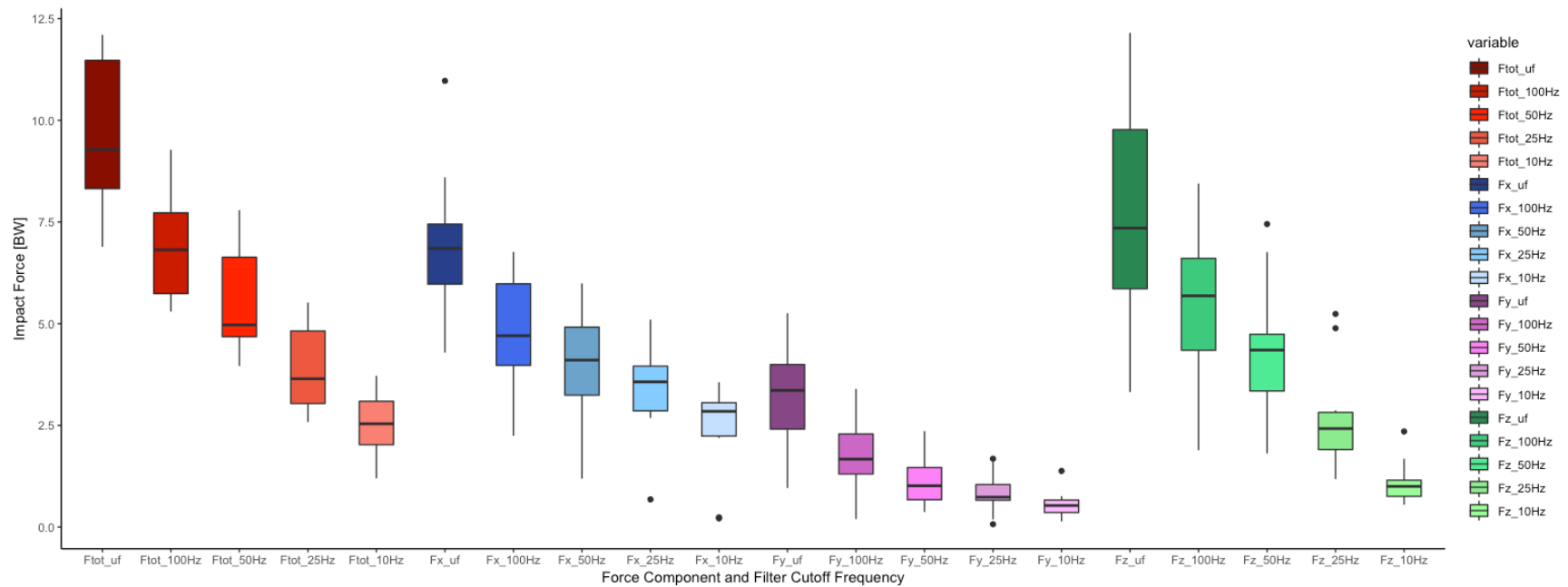
Movie 1: High speed video of an individual *Thyroptera tricolor* landing on the force plate during an experiment.

Movie 2: High speed video of *T. tricolor* landing on a natural leaf, external view.

Movie 3: High speed video of *T. tricolor* landing on a natural leaf, view from below, within the leaf tube.

Figure S1: Effects of filter cutoff frequency on measured peak impact forces (n=10 landings). Peak total force (red) and its X (vertical, blue), Y (lateral, purple), and Z (horizontal, green) components. Measurements shown for unfiltered data (darkest hues) and for data that has been filtered with a 2nd order lowpass Butterworth filter at cutoff frequencies of 100 Hz, 50 Hz, 25 Hz, and 10 Hz (decreasing cutoff frequency denoted by lighter hues). Lower cutoff frequencies attenuate impact force compared to higher cutoff frequencies and unfiltered data. In all cases, X (vertical) and Z components (horizontal into the landing plate) contribute most to the total force; however, at cutoff frequencies ≤50 Hz the attenuation is more dramatic for the Y and Z components. Boxplots show the median (horizontal line) and interquartile range (upper and lower bounds of the box); outliers indicated by points.
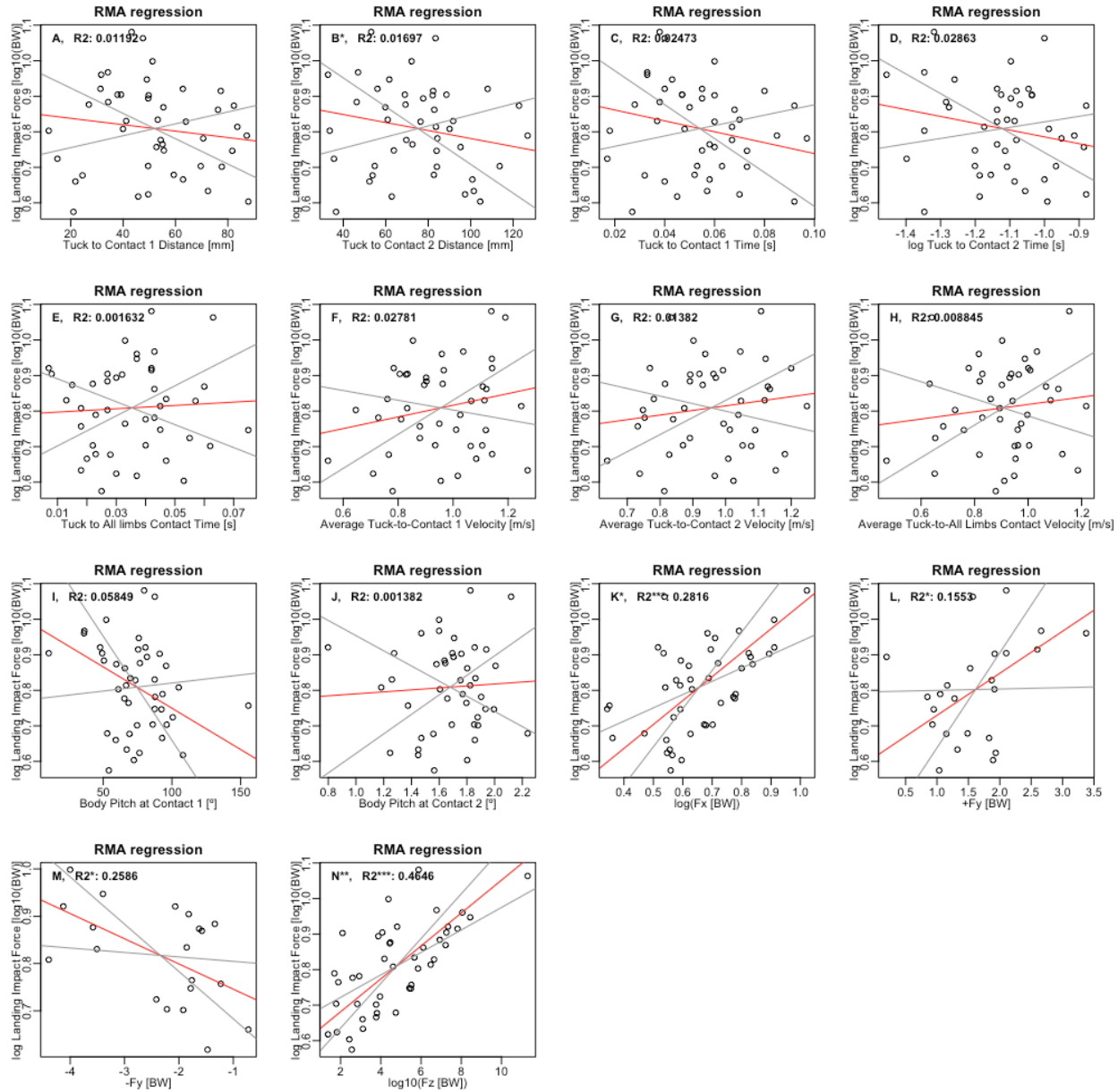
Figure S2: Model II Ranged Major Axis regressions for peak total impact force against various kinematic measurements. Red lines show the regression with 95% CI shown in black lines. R^2 is given for each regression in each panel (n=14 individuals). Points represent each landing. Slopes that differ significantly from zero are indicated by asterisks next to plot letters; significant R2 values are also indicated by asterisks. Kinematic measurements include (A) the distance between the bat's position at tuck onset to its position at the time of first limb contact; (B) the distance between its position at tuck onset and second limb contact; (C) the elapsed time between tuck onset and first limb contact; (D) the elapsed time between tuck onset and second limb contact; (E) the elapsed time between tuck onset and all limbs contact; (F) the average velocity between tuck onset and first limb contact; (G) the average velocity between tuck onset and second limb contact; (H) the average velocity between tuck onset and all limbs contact; (I) body pitch angle at the time of first limb contact; (J) body pitch at the time of second limb contact; (K) F_x; (L) $+F_y$; (M) - F_y; and (N) F_z. Other than the components of F_{tot}, no measured variables were significantly correlated with peak 3D landing impact force.